Porphyrin–Diindenothieno[2,3-*b*]thiophene Alternating Copolymer—A Blue-Light Harvester in Ternary-Blend Polymer Solar Cells

Yu-Chun Wu,[1] Yi-Hsiang Chao,[1] Chien-Lung Wang,[1] Chun-Ta Wu,[1] Chain-Shu Hsu,[1] Yu-Ling Zeng,[2] Ching-Yao Lin[2]

[1]Department of Applied Chemistry, National Chiao Tung University, 1001 Ta Hsueh Road, Hsinchu 30010, Taiwan
[2]Department of Applied Chemistry, National Chi Nan University, 1 University Road, Puli, Nantou 54561, Taiwan
Correspondence to: C.-S. Hsu (E-mail: cshsu@mail.nctu.edu.tw) or C.-Y. Lin (E-mail: cyl@ncnu.edu.tw)

Received 16 July 2012; accepted 31 July 2012; published online 14 September 2012
DOI: 10.1002/pola.26340

ABSTRACT: Porphyrin, despite chosen by Nature as light harvesting units, hasn't revealed its full potentials as a structural unit in porphyrin-incorporated polymers (PPors). A novel PPor was synthesized to investigate the origins of the low performances of PPor-based polymer solar cells (PSCs). The polymer features broad absorption in the blue-light region, because the diindenothieno[2,3-*b*]thiophene (DITT) unit extended the conjugation in the polymer backbone. PPor-DITT/$PC_{71}BM$ based PSCs have a high V_{oc} (0.79 V). Their low J_{sc} and fill factor (FF) were attributed to the un-optimized morphology, as indicated by the photoluminescence quenching and atomic force microscopy (AFM) experiments. Using PPor-DITT as a blue-light harvesting dopant in an amorphous host leverage the strong 400–550 nm absorption of PPor-DITT and circumvent the difficulties in reaching optimized morphology in the PPor/PCBM thin films. An addition of 2 wt % of PPor-DITT in ternary-blend PSCs resulted in a 10 % increase of external quantum efficiency (EQE) in the blue-light region. However, in a crystalline host, the dopant decreased the crystallinity of the host and led to large drops in FF and power conversion efficiencies (PCEs). The study provides an alternative route and expands the application of PPors in PSCs as a blue-light harvester in ternary-blend PSCs using amorphous polymers as host. © 2012 Wiley Periodicals, Inc. J Polym Sci Part A: Polym Chem 50: 5032–5040, 2012

KEYWORDS: blends; bulk heterojunction; conjugated polymers; morphology; polymer blends; porphyrin; solar cells

INTRODUCTION Technology of effectively utilizing solar energy is regarded as one of the most important issues in this century, as it will offer a clean, inexhaustible, and environmentally friendly energy source. Polymer solar cell (PSC) is a promising candidate for the solar radiation-to-electricity conversion process. It has drawn great attentions due to their potential advantages in producing large-area, lightweight, and flexible photovoltaic devices using low-cost solution processes.[1–4] Bulk heterojunction (BHJ) PSCs fabricated by blending p-type conjugated polymer as a donor (D) material and n-type fullerene-derivative as an acceptor (A) material in the active layer is one of the most useful device architectures, which attain both maximum internal donor–acceptor (D–A) interfacial area for efficient charge separation and bicontinuous network for the transport of charge carriers.[5–7] To achieve high power conversion efficiencies (PCEs), molecular structures of polymers are modified to modulate their highest occupied molecular orbital (HOMO) and lowest unoccupied molecular orbital (LUMO) energy levels to optimal values. Conjugated polymers with deep-lying HOMOs are advantageous in generating large open-circuit voltage (V_{oc}),[8–11] whereas the LUMO energy level must be at least 0.3–0.4 eV higher than the LUMO energy level of fullerene-derived acceptor for effective electron transfer.[12,13]

As an essential light-harvesting moiety in natural photosynthetic systems, porphyrin derivatives, which features rigid, two-dimensional planar π-conjugated structure, intense Soret band absorption, tunable optical and redox properties by appropriate metalation,[14,15] and ultrafast photoinduced electron transfer to fullerene,[16,17] are attracting structure units to be incorporated into conjugated polymers. So far, the exploration of main-chain porphyrin-incorporated polymers (PPors) used in PSC applications remains at its early stage. The major obstacles come from the low J_{sc} and FF of these PPor-based PSCs, which are mainly attributed to the strong yet narrow absorption bands of the PPors, and the unoptimized morphologies in the PPor/[6,6]-phenyl-C61-butyric acid methyl ester ($PC_{61}BM$) active layer. The averaged J_{sc} and FF of the PSCs fell in the rage of 0.12–5.03 mA cm^{-2} and

Additional Supporting Information may be found in the online version of this article.

0.24–0.39, respectively, which limited the maximum PCE of the PSCs to 1%.[18–23] Improving J_{sc} by broadening the absorption band and light-harvesting abilities of PPors were attempted. Zhan and coworkers[18] enhanced the coplanarity of the PPor conjugated backbone and extending the conjugation length by easing the steric hindrance among the in-chain porphyrin units. Tan et al.[19] reported random copolymers containing porphyrins, thiophenes, and 2,1,3-benzothiadiazole moieties with wide absorption band from 450–750 nm. Djurišić and coworkers[20] also reported platinum polyyne polymers containing zinc porphyrinate chromophores, showing a J_{sc} up to 3.42 mA cm^{-2} and PCE up to 1.04%. Although broader absorption spectra were successfully demonstrated, significant enhancement in the J_{sc} of the resulted PSCs was not reached. Thus, the mechanism of the unsatisfactory J_{sc} of PPor-based PSCs is not simply caused by the inefficient harvesting of solar radiation and remains unclear. Recently, instead of using porphyrin as a main-chain D unit in D–A conjugated polymers, Xiaoyu Li, Yongfang Li, and Haiqiao Wang's groups synthesized an edge-fused quinoxalino[2,3-*b*]porphyrin moiety as a novel A units. Through copolymerized the unit with carbazole-based D moiety, the resulting D–A conjugated polymers with laterally extended porphyrin units exhibits broad absorption spectrum from 400 to 750 nm and reached J_{sc} of 8.32 mA cm^{-2}, FF of 0.45, and PCE of 2.53.[24]

In fact, among all the physical properties of these PPors, the most pronounced and common feature is their exceptional strong Soret band absorption. Thus, leveraging this strength of PPors is expected to enhance the solar radiation-to-electricity conversion at blue-light region in the conventional binary polymer-fullerene system and may circumvent the poor FF of the PPor-contained PSCs. In this study, we demonstrate a novel concept of using a newly synthesized PPor, PPor-diindenothieno[2,3-*b*]thiophene (PPor-DITT; Scheme 1), as a blue-light harvesting dopant in a ternary-blend PSC. To expand the absorption in the blue-light region, the DITT comonomer unit is incorporated into the PPor conjugated backbone. The thermal, optical, and electrochemical properties of the PPor-DITT have been characterized, and the BHJ PSCs utilizing blends of PPor-DITT/[6,6]-phenyl-C_{71}-butyric acid methyl ester ($PC_{71}BM$) were fabricated to investigate the intrinsic photovoltaic properties of PPor-DITT. In addition, the origin of the low J_{sc} and FF of the PPor-DITT/$PC_{71}BM$ binary-blend PSCs are elucidated via photoluminescence (PL) quenching and morphological studies. To ensure efficient exciton dissociation and avoid charge trapping in a ternary-blend system, the prerequisite is to carefully design a cascade energy levels alignment among the components.[25–28] A crystalline conjugated polymer, P3HT, and an amorphous low-band-gap polymer, PTPTPTDPP (Fig. 1) were chosen as the host donor polymers, because first, their HOMO and LUMO energy levels form an effective cascade energy level alignment between PPor-DITT and $PC_{71}BM$; and second, the crystalline and amorphous natures of the host polymers were observed to be a critical factor in the FF of the resulting PSCs. PSCs containing ternary blends in a device configuration indium tin oxide (ITO)/poly(3,4-ethylenedioxythiophene):poly(styrenesulfonate) (PEDOT:PSS)/PPor-DITT:P3HT:$PC_{71}BM$/Ca/Al [ternary blend 1 (TB1)] and ITO/PEDOT:PSS/PPor-DITT:PTPTPTDPP:$PC_{71}BM$/Ca/Al (TB2) were fabricated and characterized.

EXPERIMENTAL

Measurement and Characterization

^{1}H NMR spectrum was recorded on a Varian-300MHz spectrometer. Gel permeation chromatography (GPC) was measured using a Viscotek GPC system equipped with a Viscotek T50A differential viscometer and Viscotek LR125 laser refractometer. Three 10-cm American Polymer columns were connected in series in the order of decreasing pore size (10^5, 10^4, and 10^3 Å); polystyrene standards were used for calibration, and THF was used as the eluent. Differential scanning calorimetry (DSC) was performed on a TA Q200 Series DSC and operated at a scan rate of 10 °C min^{-1}. Thermogravimetric analysis (TGA) was carried out using a Perkin Elmer Pyris 7 instrument at a scan rate of 10 °C min^{-1}. UV–vis spectra were measured using an HP 8453 spectrophotometer. PL spectra were obtained using an ARC SpectraPro-150 luminescence spectrometer. The cyclic voltammograms (CVs) was conducted on a Bioanalytical System analyzer. A carbon glass coated with a thin polymer film was used as the working electrode and an Ag/AgCl as the reference electrode, whereas 0.1 M tetrabutylammonium hexafluorophosphate in acetonitrile was used as the electrolyte. The CV curves were calibrated using ferrocene as the standard, whose oxidation potential is set at −4.8 eV with respect to zero vacuum level.

Fabrication of Photovoltaic Devices

ITO/glass substrates were cleaned sequentially in the ultrasonic bath of detergent, deionized water, acetone, and isopropyl alcohol for 15 min. The substrates were then covered by a 30-nm thick layer of poly(3,4-ethylenedioxythiophene):poly(styrenesulfonate) (PEDOT:PSS, Al4083 provided by H. C. Stark) by spin-coating. After annealing in air at 150 °C for 30 min, the samples were cooled down to room temperature. All the polymers were dissolved in orthodichlorobenzene, and [6,6]-phenyl-C_{71}-butyric acid methyl ester ($PC_{71}BM$, purchased from Nano-C) was added to reach the desired ratio. The solution was then heated at 70 °C for 1 h and stirred overnight at room temperature. The solution was filtered through a 0.45-μm filter before spin-coating, and the substrate was transferred into a glove box. The active layer was then spin-cast at different spin rates to achieve the optimized device performance. The experimental conditions are listed in Table S1, Supporting Information. No thermal annealing was treated for PPor-DITT/$PC_{71}BM$ binary blend and PPor-DITT/PTPTPTDPP/$PC_{71}BM$ ternary blend. The ternary blend of PPor-DITT/P3HT/$PC_{71}BM$ was annealed at 150 °C for 15 min. The spin rate is set at 1000 rpm. The cathode made of calcium (35 nm) and aluminum (100 nm) were evaporated through a shadow mask under a base pressure ($<10^{-6}$ Torr). Finally, the devices were encapsulated, and *J–V* curves were measured in air. Each device is constituted of 4 pixels defined by an active area of 0.04 cm^2.

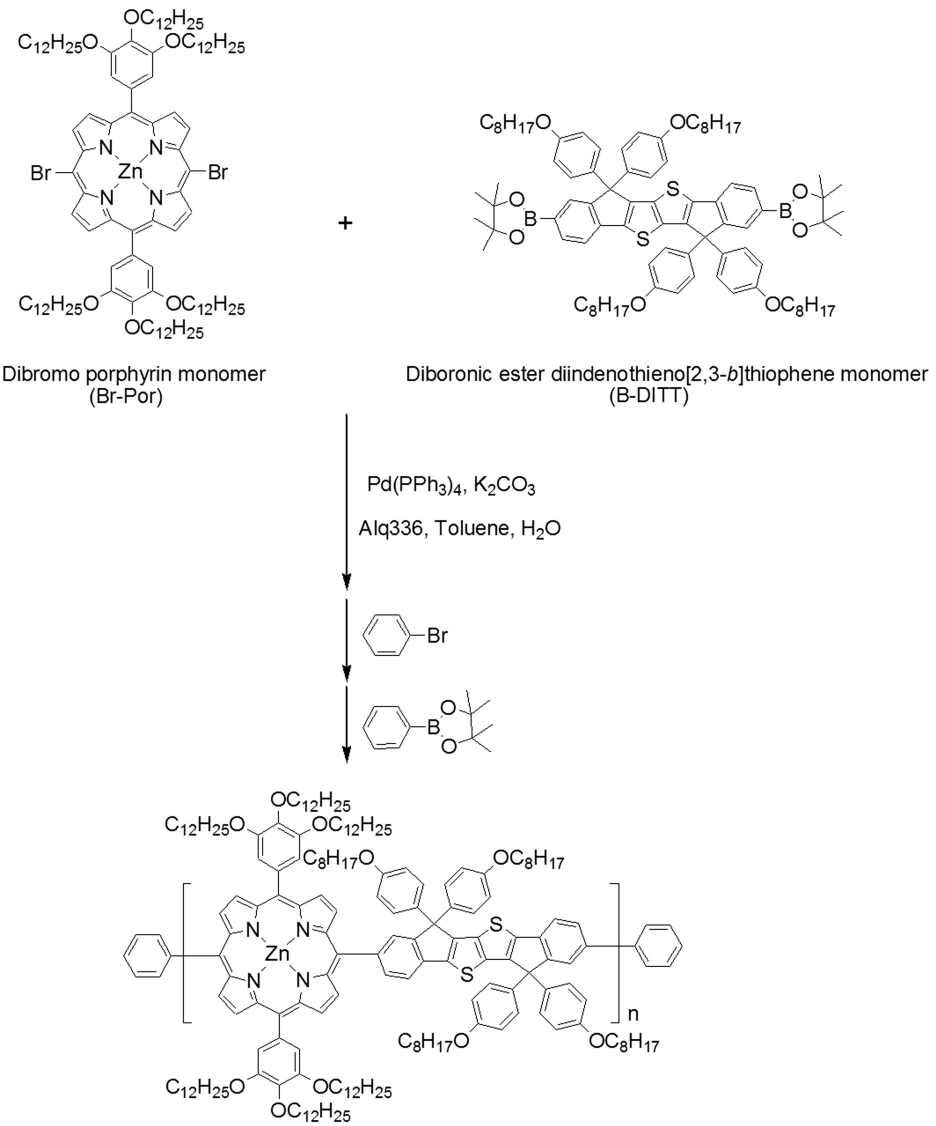

SCHEME 1 Synthetic route of PPor-DITT.

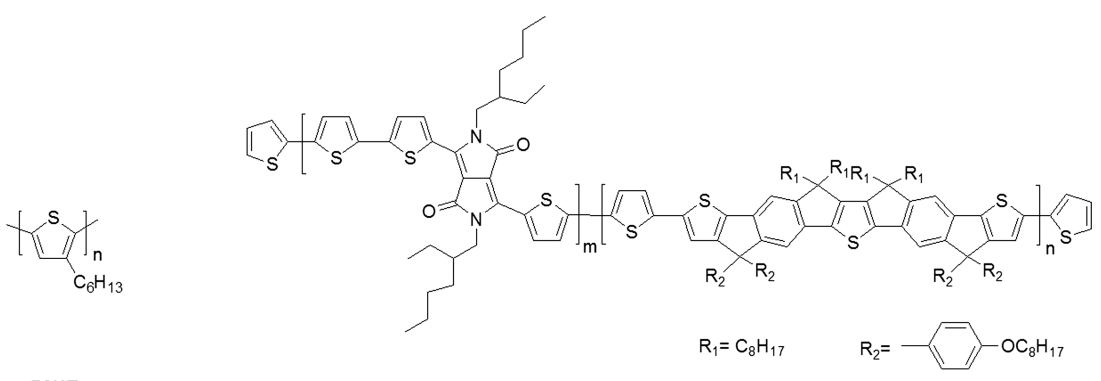

FIGURE 1 Chemical structures of P3HT and PTPTPTDPP.

Characterization of Photovoltaic Devices

The devices were characterized under the irradiation of AM 1.5 G simulated light with intensity 100 mW cm^{-2}. Solar illumination conforming the JIS Class AAA was provided by a SANEI Electric 300 W solar simulator equipped with an AM 1.5 G filter. The light intensity was calibrated with a Hamamatsu S1336-5BK silicon photodiode. Current–voltage (*J–V*) characteristics of PSC devices were obtained by a Keithley 2400 sourcemeter. The performances presented in this article are the average of 4 pixels of each device. IPCE spectra were measured using a lock-in amplifier with a current preamplifier under short-circuit conditions with illumination by monochromatic light from a 250 W quartz-halogen lamp (Osram) passing through a monochromator (Spectral Products CM110).

Synthesis of the Alternating Copolymer-PPor-DITT

All reagents and chemicals were purchased from commercial sources (Aldrich, Lancaster, or TCI) and used without further purification. The synthetic route of PPor-DITT is shown in Scheme 1. The monomers Br-Por (5,15-dibromo-10,20-bis(3,4,5-tris(dodecyloxy)phenyl) Zinc(II) porphyrin) and B-DITT (diboronic ester diindenothieno[2,3-*b*]thiophene) in Scheme 1 were synthesized according to the previous literature.[18,29,30]

Synthesis of PPor-DITT

To a 50-mL round-bottomed flask, Br-Por (179.0 mg, 0.1 mmol), B-DITT (139.0 mg, 0.1 mmol), $Pd(PPh_3)_4$ (2.3 mg, 2×10^{-3} mmol), K_2CO_3 (41.5 mg, 0.3 mmol), Aliquant 336 (10.0 mg, 0.025 mmol), degas toluene (17 mL), and degas H_2O (3 mL) were introduced. The reaction mixture was stirred at 90 °C under nitrogen for 72 h. The end-capping reagent bromobenzene (1 equiv) was added to the solution and stirred for 1 day, and then another end-capping reagent 4,4,5,5-tetramethyl-2-phenyl-1,3,2-dioxaborolane (1 equiv) was added to the solution and stirred for another 1 day. After cooling to room temperature, the solution was added into methanol dropwise. The precipitate was collected by filtration and washed by Soxhlet extraction with hexane and methanol sequentially for 2 days. The residual was collected by dissolving in THF. The Pd-thiol gel (Silicycle) was added to above THF solution to remove the Pd catalyst. After filtration and removal of the solvent, the polymer was redissolved in THF again and added into methanol to precipitate out. After drying under vacuum for 1 day, the polymer was obtained as a brown powder (108 mg, 38%).

GPC (THF, polystyrene standard) M_n = 6900 g mol^{-1}, M_w = 12,700 g mol^{-1}, PDI = 1.85. ^{1}H NMR (300 MHz, $CDCl_3$, δ): 9.17–8.90 (br, 8H, pyrrolic-H), 7.61–6.81 (br, 26H, Ar-H), 4.37–4.20 (br, 12H, —OCH_2—), 4.08–3.69 (br, 8H, —OCH_2—), 2.50–0.71 (br, 198H, alkyl-H).

RESULTS AND DISCUSSION

Synthesis and Thermal Properties of PPor-DITT

PPor-DITT was polymerized from the comonomers, Br-Por and B-DITT, by Suzuki coupling reaction,[31–34] as shown in Scheme 1. The polymer is highly soluble in common organic solvents, such as chloroform, toluene, and chlorobenzene. The number-average molecular weights (M_n), weight-average molecular weights (M_w), and polydispersity index of PPor-DITT are 6.9 kDa, 12.7 kDa, and 1.85, respectively. The 5% weight loss temperature of PPor-DITT (T_d) is at 375 °C determined by TGA as shown in Figure S2, Supporting Information. The T_d value of PPor-DITT is higher than 350 °C, indicating a sufficient thermal stability for the PSC applications. The DSC thermograms of PPor-DITT in Figure S3, Supporting Information, indicates a glass transition temperature (T_g) at 53 °C.

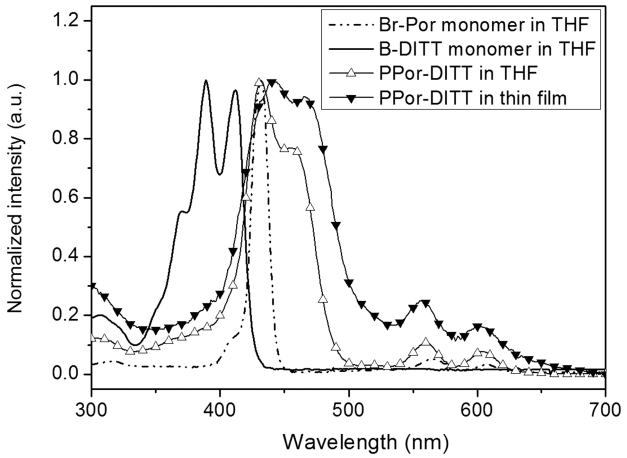

FIGURE 2 UV–vis absorption spectra of PPor-DITT and the monomers.

Optical Properties

Figure 2 shows the UV–vis absorption spectra of PPor-DITT and the comonomers (Br-Por and B-DITT) in THF. As expected, Br-Por and PPor-DITT share a sharp Soret band at 432 nm and weak Q-bands at 564 and 602 nm. The B-DITT monomer revealed the absorption band with clear vibronic structure in the region of 330–430 nm. The absorption band of B-DITT is not observed in the absorption spectrum of PPor-DITT, and the Soret band of PPor-DITT (400–500 nm) covers much broader than Br-Por, indicating that the comonomer unit, DITT, effectively extended the conjugation of the conjugated backbone. In the solid film of PPor-DITT, the Soret band further extended to 550 nm (Fig. 2). The broadened Soret band, as well as stronger Q-bands, may be attributed to a closer packing of the polymers in the solid state. Thus, via incorporation of DITT units into the PPor backbone, an alternating copolymer (PPor-DITT) covering widely in the blue-light region and suitable to be used as the blue-light harvester is obtained.

Electrochemical Properties

Figure S4 Supporting Information, shows CVs of PPor-DITT in the oxidation process. The HOMO energy level of PPor--DITT was calculated from the onset oxidation potentials (E_{ox}^{onset}), and the LUMO energy level was approximately estimated by subtracting the optical band-gap values (E_g^{opt}) from the HOMO level. The E_g^{opt} deduced from the absorption onset were determined to be 2.34 eV for the Soret band and 2.12

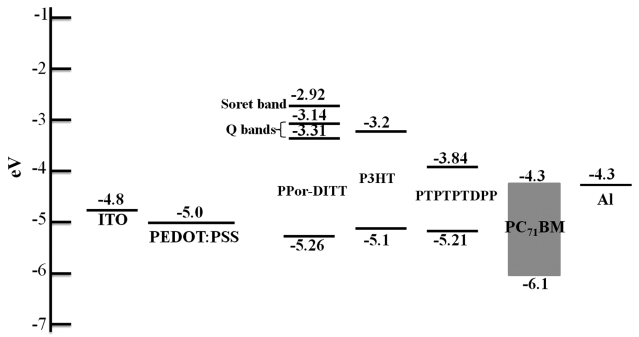

FIGURE 3 Band diagram for the donor polymers and $PC_{71}BM$.

and 1.95 eV for the Q-bands in the solid state. Therefore, the energy level of HOMO was estimated to be −5.26 eV, whereas the LUMO energy levels were calculated to be −2.92 eV for the Soret band and −3.14 and −3.31 eV for the Q-bands. With this result, to form a cascade energy level alignment and attain effective charge transfer in the ternary-blend system, the well-known crystalline P3HT and a well-performed amorphous low-band polymer PTPTPTDPP[35] were chosen as the host polymers in the ternary-blend PSCs. The energy levels of all components are illustrated in Figure 3.

Photovoltaic Characteristics

BHJ PSCs of PPor-DITT in a binary-blend system were fabricated on the basis of ITO/PEDOT:PSS/PPor-DITT:$PC_{71}BM$/Ca/Al configuration, and the characteristics were measured under AM 1.5 G illumination at 100 mW cm^{-2}. The *J–V* curve of the PSC is shown in Figure 4(a). With PPor-DITT/$PC_{71}BM$ at the optimized blend ratio of 1:3, a PCE of 0.78%, with a V_{oc} of 0.79 V, a J_{sc} of 2.98 mA cm^{-2}, and a FF of 0.33 were obtained, as listed in the inset of Figure 4(a). Figure 4(b) presents the external quantum efficiency (EQE) spectrum of the device. A broad band around the 400–550 nm matched the absorption of PPor-DITT indicating that the PPor-DITT/$PC_{71}BM$ blend has the ability to carry out solar radiation-to-current conversion in the UV to blue visible light region. However, the maximum EQE values are around 20%, and the band does not extend to long-wavelength region, which limited the J_{sc} and PCE of the PPor-DITT based PSCs.

Identical to the results in the literature, the performance of the PPor-DITT based PSCs is also limited to the J_{sc} and PCE, though V_{oc} as high as 0.79 V has been successfully reached. To further investigate this common obstacle, the PL quenching experiments and the AFM topology of PPor-DITT/$PC_{71}BM$ blend were studied. As shown in Figure 5(a)the PL emission band of pristine PPor-DITT located between 600–750 nm, and the emission is completely quenched in the thin-film of PPor-DITT/$PC_{71}BM$ blend. The results indicate that the electron transfer from the photoexcited PPor-DITT to $PC_{71}BM$ can effectively take place, and the generation of charge carriers in the blend should be efficient. Similar efficient processes of generating long-lived charge carriers ($Por^{+\cdot}$fullerene$^{-\cdot}$) from photoexcited porphyrin-fullerene dyad have been reported and well-studied.[16,17] However, the AFM image of the PPor-DITT/$PC_{71}BM$ thin-film [Fig. 5(b)] shows a featureless smooth topography with a low roughness of 0.32 nm. The morphology may cause inefficient charge transport in the PPor-DITT/$PC_{71}BM$ blend, because the ideal interpenetrating bicontinuous network was not reached.[36–38] So far, all the PPor based PSCs suffered from low J_{sc} and FF, even in the copolymer systems, which cover wide UV–vis absorption range.[18,19] Our results confirmed the efficient generation of charge carriers in the PPor-DITT/$PC_{71}BM$ blend and identified one of the major factors for the low J_{sc} and FF as the inefficient charge transport in the nonideal morphology of the active layer. Therefore, further enhancement in the PPor-based PSCs may rely on the improvement of the PPor/$PC_{71}BM$ morphology, which is currently studied in our group.

To leverage the strong 400–550 nm absorption band of PPor-DITT and circumvent the difficulties in reaching optimized morphology in the PPor/PCBM thin film, PPor-DITT

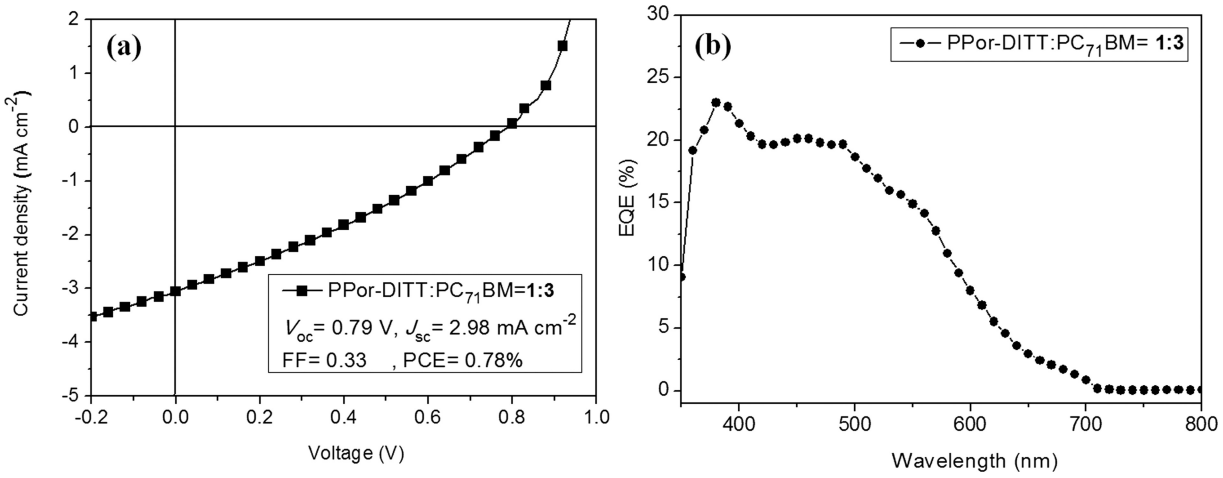

FIGURE 4 (a) *J–V* characteristics and (b) EQE spectra of ITO/PEDOT:PSS/PPor-DITT:$PC_{71}BM$/Ca/Al under illumination of AM1.5 solar simulator at 100 mW cm^{-2}.

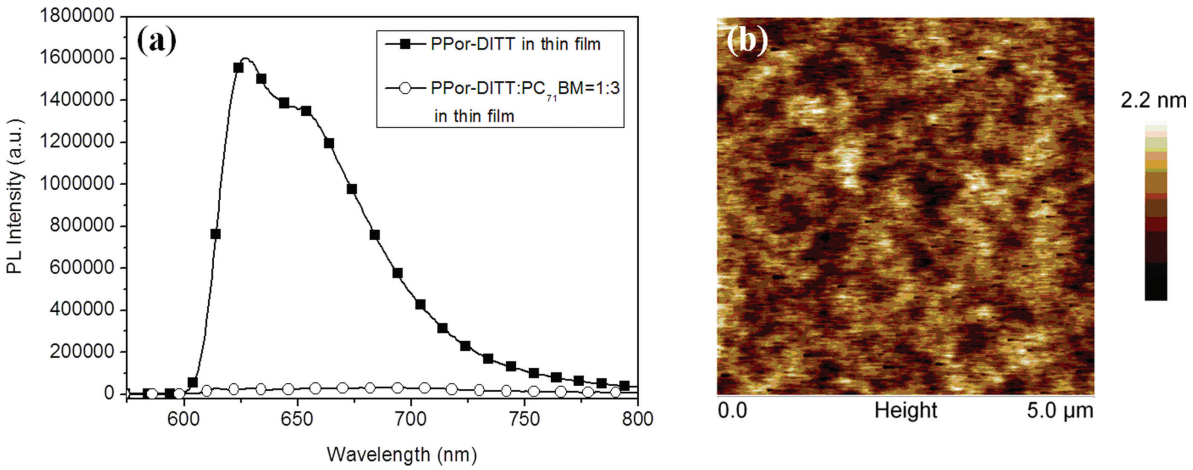

FIGURE 5 (a) PL emission spectra of PPor-DITT and PPor-DITT/$PC_{71}BM$ at the weight ratio of 1:3 in thin film. (b) Topographic AFM image (scale: 5 × 5 μm^2) of devices incorporating PPor-DITT/$PC_{71}BM$ blend at the optimized weight ratio of 1:3. Its root-mean-square roughness is determined to be 0.32 nm.

was used as blue-light harvester and an additive in a ternary-blend system. PSCs containing ternary blends in a device configuration ITO/PEDOT:PSS/PPor-DITT:P3HT:$PC_{71}BM$/Ca/Al (ternary blend 1(TB1)) and ITO/PEDOT:PSS/PPor-DITT:PTPTPTDPP:$PC_{71}BM$/Ca/Al (TB2) were fabricated. Table 1 lists the average values of J_{sc}, V_{oc}, FF, and PCE of TB1 under simulated AM 1.5G illumination (100 mW cm^{-2}) with the overall Polymer:$PC_{71}BM$ weight ratio fixed at 1:1, whereas the PPor-DITT:P3HT ratio was varied. The *J–V* curves of these devices are shown in Figure 6(a). As the ratio of PPor-DITT in the ternary blend increased, the V_{oc} values of the three-component PSCs almost remained around the reasonable value of 0.6 V. However, the values of J_{sc} decreased with the increase of PPor-DITT ratio. The results were further investigated using UV–vis absorption spectra and EQE spectra of the ternary blends. As shown in Figure 6(b)in the P3HT:$PC_{71}BM$ binary blend, an absorption maximum at 520 nm and the two absorption shoulders at 550 and 600 nm belong to the characteristic absorption band of crystalline P3HT can be clearly observed.[39] Previous study indicates that the absorption maximum shifts from 520 to 450 nm and the absorption shoulder at 550 nm disappears when the crystallinity of P3HT decreases, and the coplanarity of the conjugated backbones is distorted. The same phenomenon is observed as the PPor-DITT:P3HT ratio reached 0.2:0.8 [the triangle curve in Fig. 6(b)]. Thus, the blue-shift in the absorption spectra of the ternary blends clearly indicates that the amorphous component, PPor-DITT, although promoted the absorption at 400–500 nm, significantly decreased the crystallinity of P3HT. The decrease in J_{SC} and FF is understood as the deterioration in the photon-to-current conversion of the active layer due to the decrease of P3HT crystalline.[36] Consequently, as can be seen in Figure 6(c)the EQE spectra revealed a descending trend as PPor-DITT weight ratio increased.

Because the deterioration of J_{sc} and FF caused by the decrease in the crystalline is so severe that the possible effects brought by the PPor-DITT component could be blanked out, BHJ materials based on an amorphous conjugated polymer, PTPTPTDPP (Fig. 1) were investigated. PTPTPTDPP is a well-performed amorphous low-band-gap material for BHJ PSCs, which demonstrated a high PCE around 4.0%, when a weight ratio of PTPTPTDPP:$PC_{71}BM$ = 1:4 was used.[35] In addition, its HOMO and LUMO levels are in between the corresponding energy levels of the PPor-DITT and those of the $PC_{71}BM$. Such a cascade energy level alignment was designed, so that effective energy transfer from the photoexcited PPor-DITT dopants to the host polymer, PTPTPTDPP, may take place and facilitate the following charge separation and transport. Ternary-blend PSCs in the configuration of ITO/PEDOT:PSS/PPor-DITT:PTPTPTDPP:$PC_{71}BM$(TB2)/Ca/Al were fabricated. Table 2 lists the average values of J_{sc}, V_{oc}, FF, and PCE of TB2-based PCSs obtained under simulated AM 1.5G illumination (100 mW cm^{-2}) with the overall Polymer:$PC_{71}BM$ weight ratio fixed at 1:4, whereas the PPor-DITT: PTPTPTDPP ratio was varied. The *J–V* curves of these devices are shown in Figure 7(a). TB2-based PCSs possess higher V_{oc} values than the TB1-based PSCs due to the lower-lying HOMO level of PTPTPTDPP. Notably, on the contrary to the TB1-based PSCs, TB2-based PSCs have high FF values (>0.57) in all blending ratios (Table 2). Therefore, choosing an amorphous host polymer

TABLE 1 Photovoltaic Properties of PPor-DITT:P3HT:$PC_{71}BM$ Ternary-Blend PSCs

Polymer:$PC_{71}BM$ (w/w)	V_{oc} (V)	J_{sc} (mA cm^{-2})	FF	PCE (%)
P3HT:$PC_{71}BM$ (1:1)	0.61	7.77	0.56	2.65
PPor-DITT:P3HT:$PC_{71}BM$ (0.1:0.9:1)	0.59	7.21	0.49	2.08
PPor-DITT:P3HT:$PC_{71}BM$ (0.2:0.8:1)	0.59	6.11	0.32	1.15

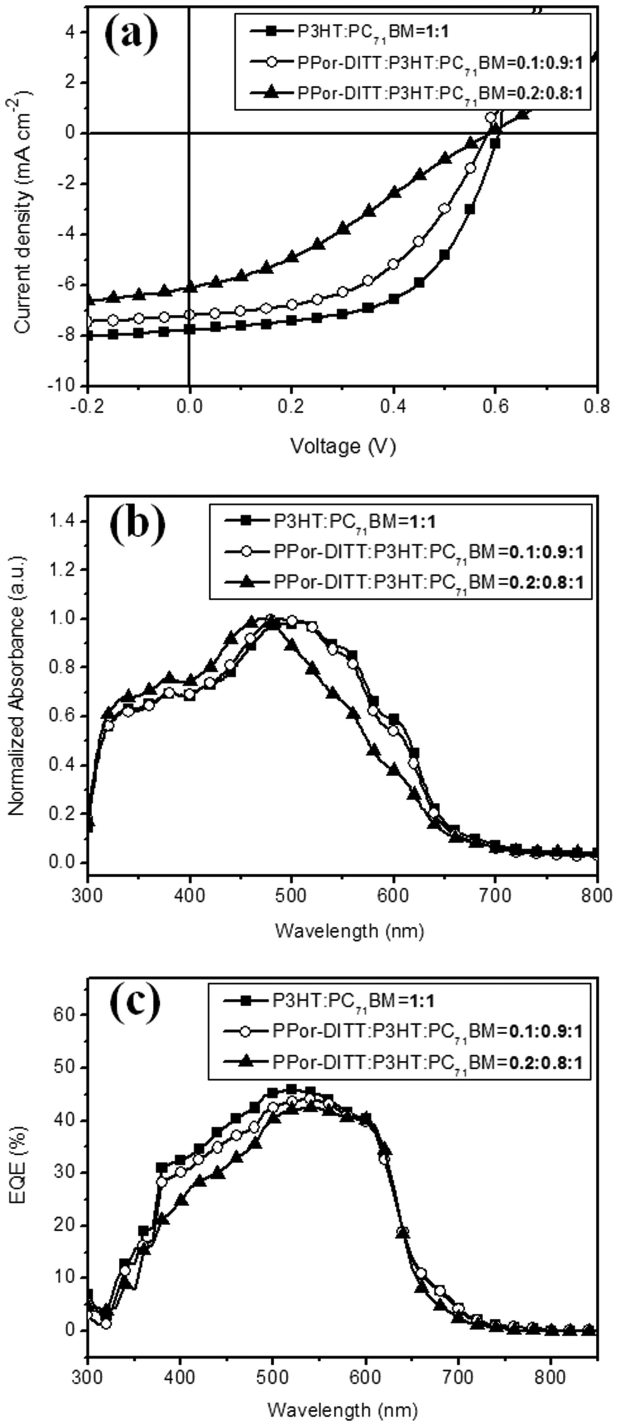

FIGURE 6 (a) *J–V* characteristics, (b) UV–vis absorption spectra, and (c) EQE spectra of PPor-DITT:P3HT:$PC_{71}BM$ ternary-blend solar cells.

avoids the drastic morphological changes accompanied with the compositional changes of the ternary blend and prevents the significant drops of FF. Most importantly, from a blending ratio of PTPTPTDPP:$PC_{71}BM$ = 1:4 to PPor-DITT:PTPTPTDPP:$PC_{71}BM$ = 0.1:0.9:4, an addition of 2 wt % of PPor-DITT, resulted in an averaged 10% increase of EQE in the region of 400–450 nm [Fig. 7(c)]. Thus, the PPor-DITT dopant at

TABLE 2 Photovoltaic Properties of PPor-DITT:PTPTPTDPP:$PC_{71}BM$ Ternary-Blend PSCs

Polymer:$PC_{71}BM$ (w/w)	V_{oc} (V)	J_{sc} (mA cm^{-2})	FF	PCE (%)
PTPTPTDPP:$PC_{71}BM$ (1:4)	0.70	9.35	0.60	3.93
PPor-DITT:PTPTPTDPP:$PC_{71}BM$ (0.1:0.9:4)	0.72	7.98	0.59	3.39
PPor-DITT:PTPTPTDPP:$PC_{71}BM$ (0.2:0.8:4)	0.72	6.52	0.57	2.68

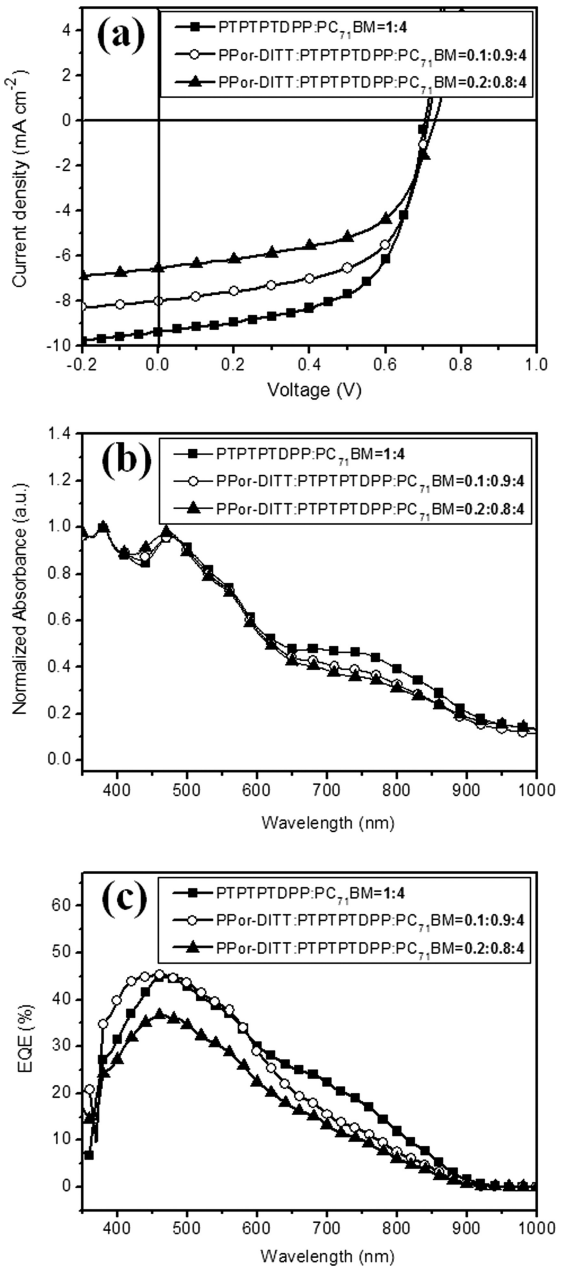

FIGURE 7 (a) *J–V* characteristics, (b) UV–vis absorption spectra, and (c) EQE spectra of PPor-DITT:PTPTPTDPP:$PC_{71}BM$ ternary-blend solar cells.

low concentration can effectively enhance the photo-to-current conversion in the blue-light region. Nevertheless, as shown in Figure 7(b)the intramolecular charge transfer absorption band of PTPTPTDPP decreased as the fraction of PPor-DITT raised, which led to a decrease in the overall J_{sc} output and PCE of the PSC (Fig. 7). Further raise of the fraction of PPor-DITT to a blend ratio of PPor-DITT:PTPTPTDPP:$PC_{71}BM$ = 0.2:0.8:4 resulted in a significant decrease in overall EQE, which limits PPor-DITT from high dopant concentrations.

CONCLUSIONS

In summary, a novel porphyrin-based polymer, PPor-DITT, featured broad absorption in the blue-light region (400–550 nm) was synthesized and used as a blue-light harvester in the ternary-blend PSCs utilizing either a crystalline conjugated polymer (P3HT) or an amorphous one (PTPTPTDPP) as a host. The BHJ PSCs based on the binary blend of PPor-DITT/$PC_{71}BM$ at the blend ratio of 1:3 show a high V_{oc} of 0.79 V, but low J_{sc} of 2.98 mA cm^{-2} and FF of 0.33. The limited J_{sc} and FF were elucidated by PL quenching experiments and AFM topology of the PPor-DITT/$PC_{71}BM$ blend, which indicate an efficient electron transfer from the photoexcited PPor-DITT to $PC_{71}BM$ but an inefficient charge transport due to the nonideal morphology of the blend. These results identify the breakthrough of the PCE of PPor-based PSCs may rely on the optimization of the active layer morphology. The ternary-blend experiments in this study demonstrated the first example of using PPor as blue-light harvester dopant in PSC applications. The amorphous nature of PPor-DITT makes it a more suitable dopant in an amorphous host. Within the crystalline host (P3HT), PPor-DITT resulted in a significant decrease of P3HT crystalline and led to great drops in $J_{sc,}$ FF, and PCE of the PSCs. On the contrary, in the amorphous host (PTPTPTDPP), the PPor-DITT dopant effectively enhanced the photo-to-current conversion in the blue-light region, with the FF well sustained at different dopant concentrations. Drop of the J_{sc} in the PPor-DITT:PTPTPTDPP:$PC_{71}BM$ ternary-blend PSCs was attributed to the decrease of the host concentration as indicated by the EQE experiments. Further optimization of the ternary composition and morphology are under process.

ACKNOWLEDGMENTS

The authors thank the National Science Council and the "ATP Program" of the Ministry of Education, Taiwan, for financial support. They also thank Yen-Ju Cheng and Sheng-Wen Cheng for providing the B-DITT monomer.

REFERENCES AND NOTES

1 Coakley, K. M.; McGehee, M. D. *Chem. Mater.* **2004,** *16*, 4533–4542.

2 Thompson, B. C.; Fréchet, J. M. J. *Angew. Chem. Int.* Ed. Engl. **2008,** *47*, 58–77.

3 Cheng, Y. J.; Yang, S. H.; Hsu, C. S. *Chem. Rev.* **2009,** *109*, 5868–5923.

4 Chang, C. Y.; Cheng, Y. J.; Hung, S. H.; Wu, J. S.; Kao, W. S.; Lee, C. H.; Hsu, C. S. *Adv. Mater.* **2012,** *24*, 549–553.

5 Yu, G.; Heeger, A. J. *J. Appl. Phys.* **1995,** *78*, 4510–4515.

6 Halls, J. J. M.; Walsh, C. A.; Greenham, N. C.; Marseglia, E. A.; Friend, R. H.; Moratti, S. C.; Holmes, A. B. *Nature* **1995,** *376*, 498–500.

7 Yu, G.; Gao, J.; Hummelen, J. C.; Wudl, F.; Heeger, A. J. *Science* **1995,** *270*, 1789–1791.

8 Scharber, M. C.; Mühlbacher, D.; Koppe, M.; Denk, P.; Waldauf, C.; Heeger, A. J.; Brabec, C. J. *Adv. Mater.* **2006,** *18*, 789–794.

9 Brabec, C. J.; Cravino, A.; Meissner, D.; Sariciftci, N. S.; Fromherz, T.; Rispens, M. T.; Sanchez, L.; Hummelen, J. C. *Adv. Funct. Mater.* **2001,** *11*, 374–380.

10 Lenes, M.; Wetzelaer, G.-J. A. H.; Kooistra, F. B.; Veenstra, S. C.; Hummelen, J. C.; Blom, P. W. M. *Adv. Mater.* **2008,** *20*, 2116–2119.

11 Kooistra, F. B.; Knol. J.; Kastenberg, F.; Popescu, L. M.; Verhees, W. J. H.; Kroon, J. M.; Hummelen, J. C. *Org. Lett.* **2007,** *9*, 551–554.

12 Brabec, C. J.; Winder, C.; Sariciftic, N. S.; Hummelen, J. C.; Dhanabalan, A.; van Hal, P. A.; Janssen, R. A. J. *Adv. Funct. Mater.* **2002,** *12*, 709–712.

13 Halls, J. J. M.; Cornil, J.; dos Santos, D. A.; Silbey, R.; Hwang, D. H.; Holmes, A. B.; Brédas, J. L.; Friend, R. H. *Phy. Rev. B* **1999,** *60*, 5721–5727.

14 Harvey, J. D.; Ziegler, C. J. *Coord. Chem. Rev.* **2003,** *247*, 1–19.

15 Chou, J. H.; Kosal, M. E.; Nalwa, H. S.; Rakow, N. A.; Suslick, K. S. In The Porphyrin Handbook; Kadisch, K.; Smith, K. M.; Guilard, R., Eds.; Academic Press: New York, **1999;** Vol. *6*.

16 Guldi, D. M.; Luo, C.; Prato, M.; Troisi, A.; Zerbetto, F.; Scheloske, M.; Dietel, E.; Bauer, W.; Hirsch, A. *J. Am. Chem. Soc.* **2001,** *123*, 9166–9167.

17 Imahori, H.; Sakata, Y. *Adv. Mater.* **1997,** *9*, 537–546.

18 Huang, X.; Zhu, C.; Zhang, S.; Li, W.; Guo, Y.; Zhan, X.; Liu, Y.; Bo, Z. *Macromolecules* **2008,** *41*, 6895–6902.

19 Zhou, W.; Shen, P.; Zhao, B.; Jiang, P.; Deng, L.; Tan, S. *J. Polym. Sci. Part A: Polym. Chem.* **2011,** *49*, 2685–2692.

20 Zhan, H.; Lamare, S.; Ng, A.; Kenny, T.; Guernon, H.; Chan, W. K.; Djurišić, A. B.; Harvey, P. D.; Wong, W. Y. *Macromolecules* **2011,** *44*, 5155–5167.

21 Liu, Y.; Guo, X.; Xiang, N.; Zhao, B.; Huang, H.; Li, H.; Shen, P.; Tan, S. *J. Mater. Chem.* **2010,** *20*, 1140–1146.

22 Lee, J. Y.; Song, H. J.; Lee, S. M.; Lee, J. H.; Moon, D. K. *Eur. Polym. J.* **2011,** *47*, 1686–1693.

23 Xiang, N.; Liu, Y.; Zhou, W.; Huang, H.; Guo, X.; Tan, Z.; Zhao, B.; Shen, P.; Tan, S. *Eur. Polym. J.* **2010,** *46*, 1084–1092.

24 Shi, S.; Wang, X.; Sun, Y.; Chen, S.; Li, X.; Li, Y.; Wang, H. *J. Mater. Chem.* **2012,** *22*, 11006–11008.

25 Koppe, M.; Egelhaaf, H. J.; Dennler, G.; Scharber, M. C.; Brabec, C. J.; Schilinsky, P.; Hoth, C. N. *Adv. Funct. Mater.* **2010,** *20*, 338–346.

26 Huang, J. H.; Velusamy, M.; Ho, K. C.; Lin, J. T.; Chu, C. W. *J. Mater. Chem.* **2010,** *20*, 2820–2825.

27 Peet, J.; Tamayo, A. B.; Dang, X. D.; Seo, J. H.; Nguyen, T. Q. *Appl. Phys. Lett.* **2008,** *93*, 163306.

28 Khlyabich, P. P.; Burkhart, B.; Thompson, B. C. *J. Am. Chem. Soc.* **2011,** *133*, 14534–14537.

29 Cheng, Y. J.; Cheng, S. W.; Chang, C. Y.; Kao, W. S.; Liao, M. H.; Hsu, C. S. *Chem. Commun.* **2012,** *48*, 3203–3205.

30 Rosen, B. M.; Wilson, C. J.; Wilson, D. A.; Peterca, M.; Imam, M. R.; Percec, V. *Chem. Rev.* **2009,** *109*, 6275–6540.

31 Rosen, B. M.; Quasdorf, K. W.; Wilson, D. A.; Zhang, N.; Resmerita, A. M.; Garg, N. K.; Percec, V. *Chem. Rev.* **2011,** *111*, 1346–1416.

32 Leowanawat, P.; Zhang, N.; Safi, M.; Hoffman, D. J.; Fryberger, M. C.; George, A.; Percec, V. *J. Org. Chem.* **2012,** *77*, 2885–2892.

33 Leowanawat, P.; Zhang, N.; Resmerita, A. M.; Rosen, B. M.; Percec, V. *J. Org. Chem.* **2011,** *76*, 9946–9955.

34 Percec, V.; Golding, G. M.; Smidrkal, J.; Weichold, O. *J. Org. Chem.* **2004,** *69*, 3447–3452.

35 Chen, C. H.; Cheng, Y. J.; Chang, C. Y.; Hsu, C. S. *Macromolecules* **2011,** *44*, 8415–8424.

36 Ma, W.; Yang, C.; Gong, X.; Lee, K.; Heeger, A. *J. Adv. Funct. Mater.* **2005,** *15*, 1617–1622.

37 Zhao, Y.; Xie, Z.; Qu, Y.; Geng, Y.; Wang, L. *Appl. Phys. Lett.* **2007,** *90*, 043504.

38 Zhao, G.; He, Y.; Li, Y. *Adv. Mater.* **2010,** *22*, 4355–4358.

39 Yang, C.; Orfino, F. P.; Holdcroft, S. *Macromolecules* **1996,** *29*, 6510–6517.